Direct Synthesis of Nitrogen Vacancy-Enhanced Ni_3N/Ni Catalysts for Alkaline Hydrogen Evolution with High Activity and Stability

Doudou Zhang[1], Siva Krishna Karuturi[1], Kylie Catchpole[1]

[1.] Research School of Electrical, Energy and Materials Engineering, Australian National University, ACT, Australia (doudou.zhang@anu.edu.au)

Background

- Ni-nitrides and their heterostructures are particularly promising due to their high binding capabilities for the adsorbates (atomic hydrogen, protons, or water molecules) and relatively low electrical resistance.[1-2]
- Nitrides are usually synthesized by self-propagating high-temperature synthesis with nitridation at >400 °C in the presence of hazardous chemicals.[3-4]
- We report the use of an industrially-mature and eco-friendly magnetron sputtering method to directly synthesize Ni_3N/Ni with a triangular pyramidal structure enriched with N-vacancies.[5]

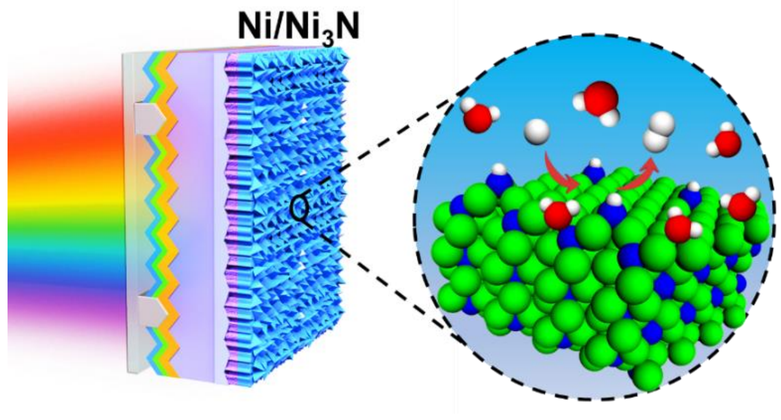

TOC. *(a) Schematic diagram of Ni_3N/Ni/Si photocathode with Ni_3N/Ni cocatalysts with N-vacancies.*

Physical Characterisation

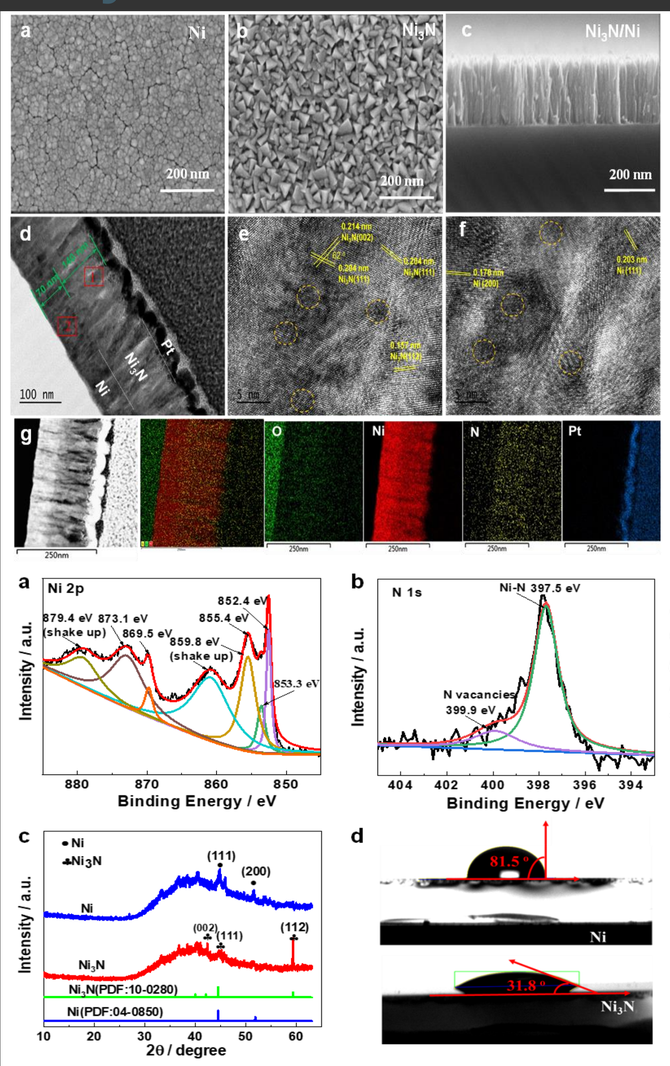

Figure 1*. Scanning electron microscopy images of (a) Ni and (b) Ni3N from top-view, and (c) Ni_3N/Ni from cross-sectional view. d) Scanning transmission electron microscopy image of Ni_3N/Ni layers with Ni3N marked as block 1 and Ni marked as block 2. (e, f) High resolution transmission electron microscopy images collected from blocks 1 and 2, respectively. (g) Transmission electron microscopy image and the corresponding elemental mappings of Ni_3N/Ni. Pt observed in the images was deposited as a protection layer during the milling process for the preparation of cross-section samples.*

- Ni film shows a nanoparticle morphology with a size of ~20 nm with visible grain boundaries and cracks, and the thickness is 70 nm.
- Ni_3N film with triangular pyramid structure morphology without cracks with thickness of 140 nm

Figure 2. *(a) X-ray photoelectron spectroscopy spectra of (a) Ni 2p 3/2 and (b) N 1s of Ni_3N. (c) X-ray diffraction patterns of Ni and Ni_3N. (d) Water contact angle measurements for Ni/FTO and Ni_3N/Ni/FTO measured after resting water droplets on the surface for 4 s.*

- The XRD patterns of Ni_3N shows weaker and broader diffraction peaks, indicating poor crystallinity or defective structure of the material.
- The much smaller contact angle on Ni_3N/FTO suggests a higher wettability for Ni3N/Ni/FTO, which could be beneficial for enhanced HER kinetics.

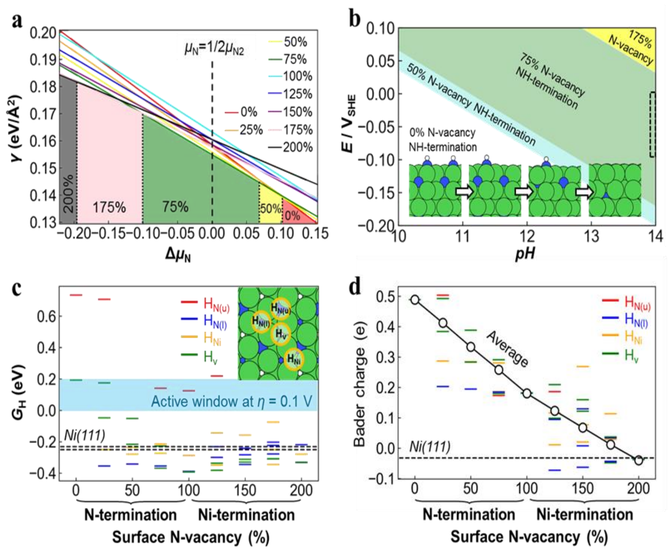

Figure 3. (a) Surface free energy (γ) of Ni_3N(001) with a varying amounts of N-vacancies as a function of surface chemical potential difference to gaseous N_2 (ΔμN). The coloured areas show the region of most stable structures under the lines with lowest γ. Black, pink, green, yellow and red lines correspond to combined N-vacancy concentrations in the surface and sub-surface layer of 200% (Ni), 175%, 75%, 50% and 0% (Ni_3N). 75% N-vacancy concentration is most stable at gaseous N_2 conditions (horizontal black dashed line). (b) Surface Pourbaix diagram of NixNyHz with N with reference to dissolved N_2. The HER working condition is 1.0 M KOH (pH≈13.8) and E = -0.1 eV, as approximately marked in the black dashed box. (c) Adsorption free energies of H* (GH) on 4 inequivalent Ni_3-hollow sites (d) Bader charge of 4 inequivalent Ni3-hollow sites exhibited by a Ni_3N (001) surface with varying degree of surface N-vacancies. Positive Bader charge values represent atoms with positive charge. The corresponding values for the Ni_3-hollow sites at Ni (111) are shown as dashed lines for comparison (the two inequivalent sites share the same value). The average values of the surface Ni atoms for each termination are marked as circles.

- Nitrogen plasma includes molecular, atomic, and ionic nitrogen ($N^{1+}$and N^{2+}) species which lead to the formation of N-vacancies.
- Using DFT calculations, the presence of N-vacancies under electrochemical working conditions which effectively enhance the adsorption of water molecules and improve the adsorption-desorption behavior of intermediate species, resulting in superior HER activity

Electrochemical and Photoelectrochemical Characterisation

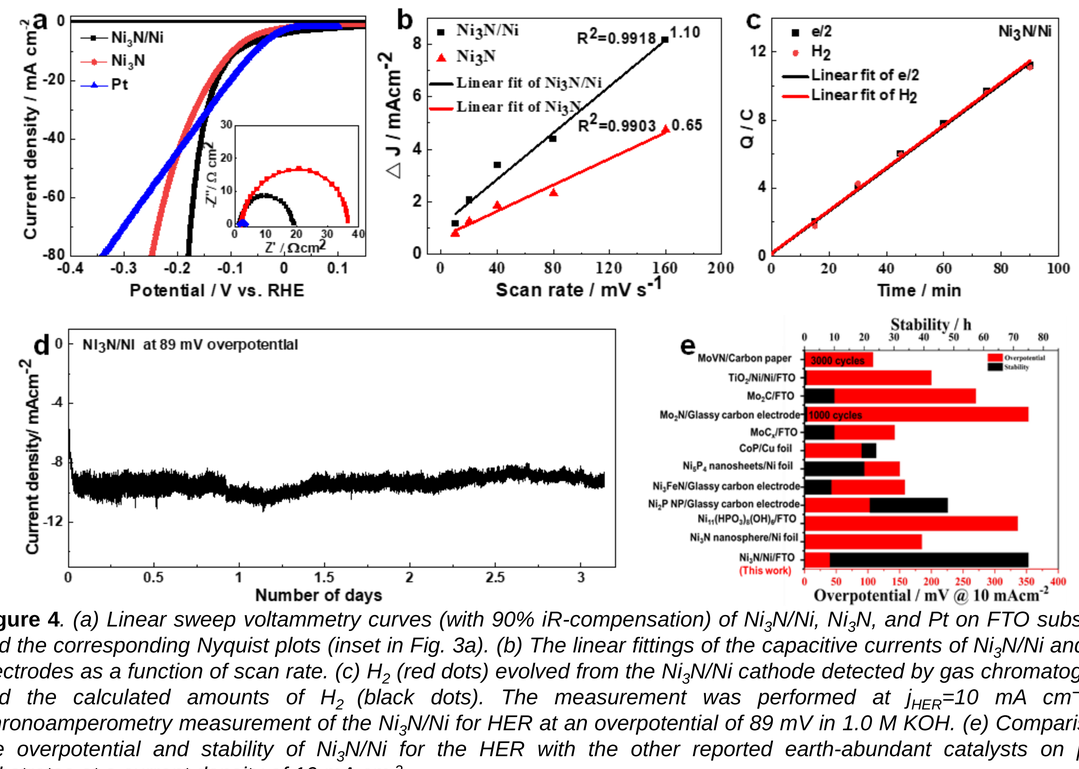

Figure 4. *(a) Linear sweep voltammetry curves (with 90% iR-compensation) of Ni_3N/Ni, Ni_3N, and Pt on FTO substrates and the corresponding Nyquist plots (inset in Fig. 3a). (b) The linear fittings of the capacitive currents of Ni_3N/Ni and Ni_3N electrodes as a function of scan rate. (c) H_2 (red dots) evolved from the Ni_3N/Ni cathode detected by gas chromatography and the calculated amounts of H_2 (black dots). The measurement was performed at j_{HER}=10 mA cm^{-2}. (d) Chronoamperometry measurement of the Ni_3N/Ni for HER at an overpotential of 89 mV in 1.0 M KOH. (e) Comparison of the overpotential and stability of Ni_3N/Ni for the HER with the other reported earth-abundant catalysts on planar substrates at a current density of 10 mA cm^{-2}.*

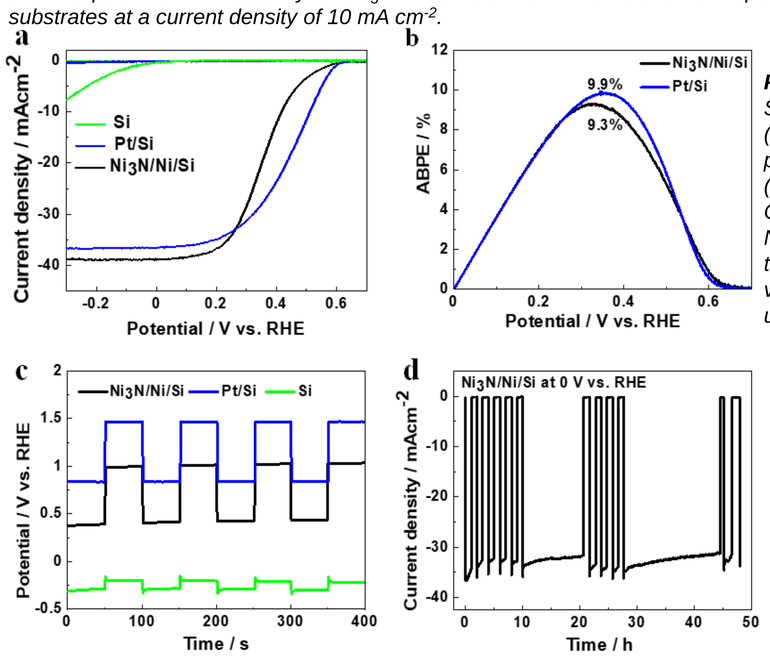

Figure 5. *(a) Linear sweep voltammetry of Si, Pt/Si and Ni_3N/Ni/Si photocathodes and (b) the corresponding applied bias-to-photon current conversion efficiency, and (c) Open-circuit potential plots. (d) Chronoamperometry measurements for the Ni_3N/Ni/Si photocathode at 0 V vs. RHE. All the measurements were performed at 0 V vs. RHE in 1.0 M KOH electrolyte (pH=14) under AM1.5G illumination (100 mW cm^{-2}).*

- The Ni_3N/Ni catalyst shows low crystallinity and good wettability, and exhibits a low overpotential of 89 mV vs reversible hydrogen electrode (RHE) at 10 mA cm^{-2} in 1.0 M KOH with an excellent stability of over 3 days.
- The application of Ni3N/Ni as a cocatalyst on Si photocathodes produces an excellent applied bias photon-to-current efficiency of 9.3% and over 50 h stability.

Conclusions

- The demonstration of earth-abundant Ni_3N/Ni catalysts with HER performance comparable to that of Pt, and directly synthesized using magnetron sputtering, i.e., without the need of a high temperature nitridation process, provides promise for application in electrochemical and photoelectrochemical solar hydrogen production.

References

[1] D. Zhang, Energy Environ. Sci., 2022, 15, 185-195
[2] R. Subbaraman et al., Science 2011, 334, 1256.
[3] D. Zhang et al., Advanced Science 2018, 5, 1801216.
[4] F. Song, Nature communications 2018, 9, 1.
[5] W.-F. Chen et al., Angew. Chem. Int. Ed. 2012, 51, 6131.
[6] D. Zhang et al., ACS Energy Letters. submitted.

Australian National University
ANU College of **Engineering & Computer Science**

This work has been supported through the Australian Renewable Energy Agency. Responsibility for the views, information or advice expressed herein is not accepted by the Australian Government.